

Maximum Rain-Rate Evaluations in Aegean Archipelagos Hellas for Rain Attenuation Modeling at Microwave Frequencies

E.A. Karagianni, C.N. Vazouras & E.H. Papageorgiou
Hellenic Naval Academy, Piraeus, Greece

A.D. Sarantopoulos
Hellenic National Meteorological Service, Eliniko, Greece

H.E. Nistazakis
National and Kapodistrian University of Athens, Athens, Greece

ABSTRACT: By utilizing meteorological data such as relative humidity, temperature, pressure, rain rate and precipitation duration at eight (8) stations in Aegean Archipelagos from six recent years (2007 – 2012), the effect of the weather on Electromagnetic wave propagation is studied. The EM wave propagation characteristics depend on atmospheric refractivity and consequently on Rain-Rate which vary in time and space randomly. Therefore the statistics of radio refractivity, Rain-Rate and related propagation effects are of main interest. This work investigates the maximum value of rain rate in monthly rainfall records, for a 5 min interval comparing it with different values of integration time as well as different percentages of time. The main goal is to determine the attenuation level for microwave links based on local rainfall data for various sites in Greece (L-zone), namely Aegean Archipelagos, with a view on improved accuracy as compared with more generic zone data available. A measurement of rain attenuation for a link in the S-band has been carried out and the data compared with prediction based on the standard ITU-R method.

1 INTRODUCTION

1.1 Humidity of the atmosphere

Water is the only substance that can be found naturally in all three states (gas, liquid, solid) in the atmosphere. Humidity is the general term to show the existence of the “water” in the atmosphere. Parameters related to atmospheric humidity levels include water vapor pressure (e), saturation vapor pressure (e_s), relative humidity (H), dry temperature (θ), precipitation height (h), precipitation time interval (t), pressure (P), water vapor density (ρ).

Water in any state affects the transmission of electromagnetic waves. When the wave passes through a humid atmospheric layer, part of its energy is reflected or scattered, another is absorbed and the rest is passing without any change. Therefore the electromagnetic wave is attenuated. The

attenuation is caused by the scattering and absorption of electromagnetic waves by drops of liquid water. The scattering diffuses the signal, while absorption involves the resonance of the waves with individual molecules of water. Absorption increases the molecular energy, corresponding to a slight increase in temperature, and results in an equivalent loss of signal energy.

Precipitation phenomena result in signal attenuation, as well as corresponding increase of the system noise temperature. Further on, rain causes cross-polarization interference in dual polarization systems. These three effects cause degradation in the received signal quality, particularly for frequencies above 10 GHz, resulting in increase of the system outage time. Hence, prediction of their influence is very important in microwave telecommunications systems design.

1.2 The raindrop

The raindrop size distribution and the drop shape relation have great variation in different precipitation conditions. In heavy precipitation phenomena the raindrop size is composed of lots of median and small raindrops rather than giant raindrops [1], [7]. Both shape and size are depending from the dynamics principles where a raindrop is deforming as it falls in air, breaking into smaller fragments. The topological change from a big drop into smaller stable fragments is accomplished within a time scale much shorter than the typical collision time between the drops [2], [3], [8]. Regarding strong precipitation phenomena, the size of a typical raindrop, is about 3 millimeters, although the typical diameter of a rain droplet is 1mm as emerged from the radar reflectivity factor Z measured in mm^6/m^3 .

1.3 The relative refractive index

When the propagation medium is a material different than air, the speed of an electromagnetic wave depends on the relative dielectric constant known as relative permittivity ϵ_r and to the relative permeability μ_r , with the following formula:

$$v = \frac{1}{\sqrt{\epsilon_r \cdot \mu_r}} = \frac{c}{\sqrt{\epsilon_r \cdot \mu_r}} \quad (2)$$

where $\epsilon = \epsilon_0 \epsilon_r$ and $\mu = \mu_0 \mu_r$, are the permittivity and permeability in F/m and H/m respectively, and ϵ_r and μ_r are the relative permittivity and permeability of the medium [6], [11].

The relative refractive index, n is defined as

$$n = \sqrt{\epsilon_r \cdot \mu_r} \quad (3)$$

Values for the relative refractive index, are presented in Figure 3 for four years observations in Skyros Island at Northwest Aegean Sea (Figure 2).

2 RAIN MODELS FOR WAVE ATTENUATION

2.1 Rain attenuation

The electromagnetic wave attenuation due to rain (the rain attenuation) is one of the most noticeable components of excess losses, especially at frequencies of 10 GHz and above. Considerable research has been carried out to model rain attenuation mathematically and to characterize rainfall throughout the world. A host of methods for estimating rain attenuation is based on the power law for specific attenuation combined with the notion of effective path length [10], [14], [15].

$$L_r = k \cdot R^\alpha \cdot L \quad (4)$$

where L_r is the rain attenuation (in dB), R is the rain rate (in mm/h), L is the effective path length (in km), and k and α are empirical coefficients, functions of

the operating frequency (f), polarization (k_h or α_h - h for horizontal polarized waves and k_v or α_v - v for vertical polarized waves) and temperature (T).

For horizontally polarized waves, k_H and α_H parameters are given in Table 1 for selected S and X band frequencies [12], [16].

Table 1. Parameters for horizontally polarized waves (h) in S and X-band.

Frequency (GHz)	$k_H(\times 10^{-3})$	α_H
2,5	0,1321	1,1209
5	0,2162	1,6969
10	12,17	1,2571

The equivalent path length depends on the angle of elevation of the communication link, the height of the rain layer (h), and the latitude of the earth station. (Figure 1)

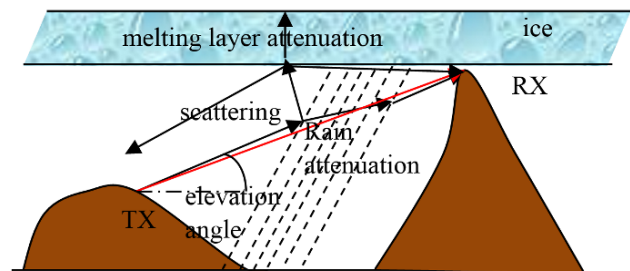


Figure 1. Path length through rain

The rain rate enters into equation 4 because it is a measure of the average size of the raindrops. When the rain rate increases that means it rains harder, the rain drops are larger and thus there is more attenuation. Also, the conversion of the radar reflectivity factor to rain rate is a crucial step in weather radar measurements. It has been common practice for over 60 years now to take for this conversion a simple power law relationship between them, using the classical exponential raindrop size distribution [17], [18].

2.2 Rain Models

Rain models differ principally in the way the effective path length L is calculated. Two rain models are widely used, the Crane model and the ITU-R model (International Telecommunication Union's Radio-communication sector). The two-component Crane model takes into account both the dense center and the fringe area of a rain cell [11], [19]. In the design of a telecommunications' link a margin is included to compensate for the effects of rain at a given level of availability. The statistical characterization of rain begins by dividing the world into rain climate zones. Within each zone, the maximum rain rate for a given probability is determined from actual meteorological data accumulated over many years.

The methods of prediction of the rain attenuation can be categorized into two groups: the physical models and the empirical models. The physical models attempt to reproduce the physical behavior involved in the attenuation processes while the

empirical methodologies are based on measurement databases from stations in different climatic zones within a given region. The empirical methods are used widely.

The factor $\gamma_r=L_r/L$ (in dB/Km), where L_r and L are defined in equation 4, is called the specific rain attenuation. One of the most widely used rain attenuation prediction methods is the empirical relationship between this specific rain attenuation γ_r (in dB/km) and the rain rate R (in mm/h) [12], [13]

$$\gamma_r = k \cdot R^\alpha \quad (5)$$

3 RAIN RATE

For the determination of the rain attenuation, the main parameter used is the rain rate R , which is expressed in mm/h. The rain rate can be described as the thickness of the precipitation layer, which felled down over the time period of one hour in the case when the precipitation is not evaporated, not soaked into the soil, and is not blown away by the wind. The evaluation of R -value is of crucial importance in the rain attenuation prediction. The rain attenuation depends on the meteorological conditions in the considered place.

3.1 Integration Time

The R -values are expressed in mm/h. Time intervals between the readings of rainfall amount in many cases are unrealistic. The period of time between the readings of the rainfall amount values is called integration time τ and it is a very important parameter, because it can significantly change the R -value. High R -values are hidden when τ is long.

As an example, we assume that it was raining for 5 minutes and the total amount of the precipitation at this time was 20 mm. For the remaining 55 minutes was not raining and during the remaining minutes of 3 hours as well. Thereby, the average R -value is 20 mm/h. On the other hand, if we count the average R for a measuring duration of 15 minutes, it will be 80 mm/h, for 10 minutes 120 mm/h and for 5 minutes it will be 240mm/h. Similarly, if we count R -value for every rainy minute, we will find that $R=240$ mm/h, since in every of those 5 minutes the amount of the precipitation was 4 mm/min. The different outcomes for the R -values make this way of counted unreliable)

3.2 The "one-minute" rain rate

Almost all rain attenuation prediction methods require one-minute integration time rain rate values.

Table 2. Rain Height in mm during 5min, 10 min, 15 min, 1h, 3h and 12h

Hellas Island	Rain Height in mm					
	5min	10min	15 min	1h	3h	12h
Mykonos	7,2	13,4	17,6	47,4	66,9	108,8
Naxos	-	0,80	7,10	18,6	38,4	38,8
Thyra	12,0	23,8	31,8	48,9	51,5	51,5
Rodos	12,1	19,6	26,4	51,3	72,1	73,2
Samos	10,0	15,1	20,0	43,7	53,7	78,3
Chios	15,3	16,2	25,9	42,0	56,0	159,0
Mytilini	8,6	12,2	16,1	31,6	40,1	67,6
Skyros	0,01	2,40	3,00	74,0	74,0	74,0

However, in our case, 5-min, 10-min, 15-min, 1-h and 12-hourly instances data are used. There are various models for conversion of (τ -min) into (1-min) rainfall statistics (see e.g. [5], [9], [10], [14]), usually based on either equal rainfall rate or equal probability approach; an example of the latter (as in [9]) results in a relationship of the form

$$R_{1 \text{ min}} = a (R_{\tau \text{ min}})^b \quad (6)$$

where $R_{\tau \text{ min}}$ is rain rate value measured in τ minutes ($\tau \geq 1 \text{ min}$) and $R_{1 \text{ min}}$ the "one-minute" rain rate value, while a and b are appropriate regression coefficients. The difficulty with such techniques is that they usually require 1-min measured data to estimate the regression coefficients, which consequently are location-specific. An alternative approach (for τ between 5 and 60 minutes) is given by the synthetic model based on software simulation suggested in Annex 3 of [23].



Figure 2. Meteorological Stations in Aegean's Islands

On the other hand, the main advantage of the "Worst-month" model which was proposed by ITU-R [12] is that only the worst-month statistics must be collected, although it is appropriate in cases when the required reliability of the radio system is other than 99.99%. This month is not necessarily the same month in different year. The fraction of time when the threshold value of rain rate (so, and rain attenuation value) was exceeded is identical to probability that the threshold value of rain rate would be exceeded [15], [19].

Table 3. Rain Rate at 0,001% and 0,01% in mm/h

Hellas Province Island (Lat/Log)	Rain Rate at 0,001% in mm/h	Rain Rate at 0,01% in mm/h
Mykonos	86,4	47,4
Naxos	-	11,0
Thyra	144,0	48,9
Rodos	145,2	51,3
Samos	120,0	43,7
Chios	183,6	42,0
Mytilini	103,2	31,6
Skyros	80,7	48,0

4 DATA ANALYSIS

Our survey is focused on those measurements referred as Aegean Archipelagos, namely, Mykonos, Naxos, Santorini, Rodos, Samos, Chios, Mytilini and Skyros islands which cover the whole northwest and northeast region of Aegean Sea.

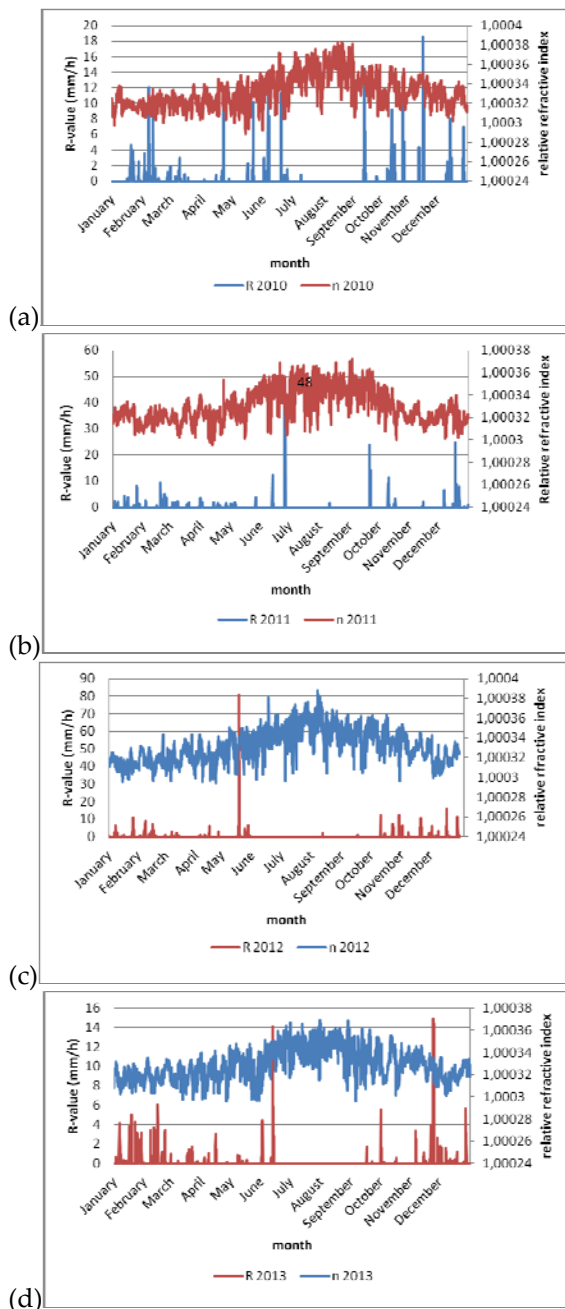


Figure 3. Rain rate and relative refractive indexes for the period January 2010 – December 2013 for Skyros Island.

The precipitation amount as a meteorological index on Skyros has a maximum value of 74 mm for the period January 2010 to December 2013. This value appeared in May 2012 for 55 minutes, giving a R-value of 81 mm/h. The day following this storm, an R-value of 43 mm/h (36 mm for 50 minutes) was observed. The next maximum values for precipitation height appeared in June 2011 (64 mm) for 1 hour and 20 minutes and in February 2012 (53 mm) for 6 hours, giving R-values at 48 mm/h and 8,8 mm/h respectively.

5 REFRACTIVITY

Another parameter to consider is the relative refractive index of the atmosphere given in equation 3, which affects the curvature of the electromagnetic wave path and graces the fading phenomenon. For example, the anomalous electromagnetic wave propagation can cause disturbances to radar work, because variation of the refractive index of the atmosphere can induce loss of radar coverage. Accurate prediction of losses due to these factors can ensure a reliability of the telecommunication system, decrease the equipment cost and protect people.

5.1 Refractive Index

The relative refractive index, n , for the troposphere, is computed by [20]

$$n = 1 + N \cdot 10^{-6} \quad (7)$$

where N is the radio refractivity expressed by:

$$N = N_{\text{dry}} + N_{\text{wet}} = 77,6 \cdot \frac{P}{T} + 3,732 \cdot 10^5 \cdot \frac{e}{T^2} \quad (8)$$

with P being the atmospheric pressure (in mbars), e the water vapor pressure (in mbars), and T the absolute temperature (in $^{\circ}\text{K}$).

This expression may be used for all radio frequencies. The relationship between water vapor pressure e and relative humidity is given by:

$$e = \frac{H \cdot e_s}{100} \quad (9)$$

where

$$e_s = EF \cdot a \cdot \exp \left[\frac{\left(\frac{b-t}{d} \right) \cdot t}{t+c} \right] \quad (10)$$

where $a=6.1121\text{mb}$ is the vapour pressure at the triple point and it has the same unites with e_s and

$$EF = 1 + 10^{-4} \cdot \left[7,2 + P \cdot \left(0,0032 + 5,9 \cdot 10^{-7} \cdot t^2 \right) \right] \quad (11)$$

where t is the temperature (in °C), P is the pressure (in mbars), H is the relative humidity (in %) e_s is the saturation vapor pressure (in mbars) at the temperature t (in °C) and the coefficients b , c and d for water for the measured temperature, are:

$b=18.678$, $c=257.14$, $d=234.5$.

Vapor pressure e in mbars is obtained from the water vapour density ρ (in g/m^3) using the equation:

$$e = \frac{\rho \cdot T}{216,7} \quad (12)$$

where ρ is given in g/m^3 .

Skyros annual averages for the period 2010 to 2013 are $N_{dry}=272$, $EF_{water}=1,001$, $e_s=20,3$, $e=13,02$, $N_{wet}=57,07$, $N=328,95$, $n=1,0003$ and $\rho=9,67$ while Naxos averages which is located south from Skyros for the same period, are $\theta=18,8^\circ C$ dry temperature, $P=1013,77$ mbars, $H=68,44\%$ relative humidity, $N=336.18$ and $\rho=11,3$.

It is noticeable that our statistics based at 12-hour measurements 6:00 and 18:00, and this for the following reason: During the 12-hour measurements, the station, recorded summed with the last 3 hour and all measurements were preceded during that 12 hour and were given separately in each 3-hour observation.

Note that the maximum value R , appeared in Naxos, on 5th of November 2013 at 06:00 UTC and this value is 55,8 mm/h, much smaller than this appeared in Skyros (81mm/h).

Table 2. Observed parameters values at a specific parameter at its minimum value (in bold).

τ minutes	H mm	P mbars	θ °C	H %	N	R mm/h
80	3,4	981,6	11,4	81	318	3
0	0	1021,8	-0,6	65	310	0
10	0	1006,9	32,4	19	293	0
0	0	1006	27,4	19	288	0

Table 3. Observed parameters values at a specific parameter at its maximum value (in bold).

τ minutes	H mm	P mbars	θ °C	H %	N	R mm/h
720	20,8	1016,9	20,8	88	336	2
0	0	1035	2,4	58	212	0
0	0	1000,9	35,2	31	321	0
0	0	1020,7	22	100	380	0
0	0	1013,3	29	78	388	0
55	74	1009,9	15,4	88	341	81

In tables 2 and 3, observed parameters values are presented, for precipitation time interval (τ), precipitation height (h), pressure (P), dry temperature (θ), relative humidity (H), refractivity (N) and Rain-Rate (R) at a specific parameter at its minimum (Table 2) and maximum value (Table 3) respectively. In strong precipitation phenomena, as it

is shown in figure 4, the temperature decreases and the relative humidity increases. The relative refractive index will be increased as it is proportional to the water vapor pressure (which in turn is proportional to the relative humidity) and inversely proportional to temperature. The same phenomenon is observed when the precipitation has very small rain-rates although the temperature, pressure relative humidity changes - and consequently refractivity and relative refractive index changes - occur a couple of hours later as it is presented in the diagram of figure 5.

6 DISCUSSION

The main models for calculation of electromagnetic wave attenuation due to atmospheric humidity and heavy precipitation phenomena, were revised. In Aegean Sea, Hellas, when the reliability of the radio system of 99,99% is required, R -value equals to approximately 50 mm/h. The attenuation of horizontally polarized electromagnetic waves is greater than the attenuation of vertically polarized electromagnetic waves. The dependency of the average specific electromagnetic wave attenuation due to rain on the operating frequency was determined.

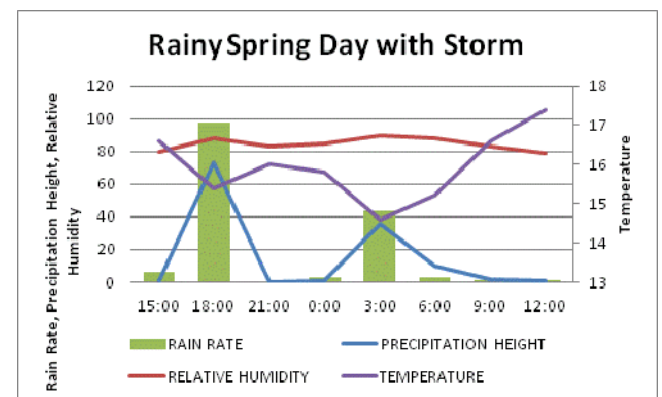


Figure 4. Hourly parameters presentation on a rainy day with storms in May 2012 at Skyros island

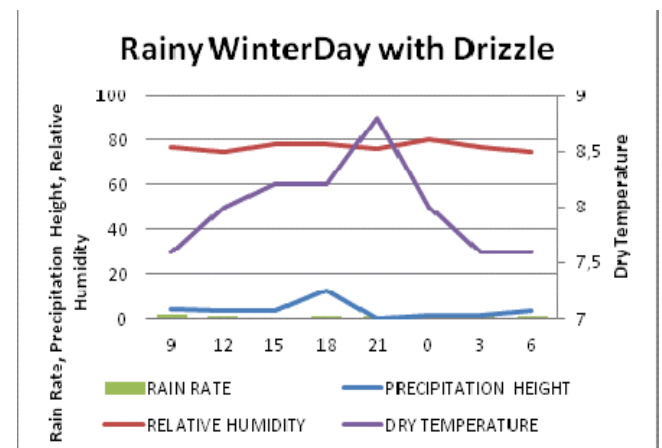


Figure 5. Hourly parameters presentation on a drizzle day at the end of January 2011 at Skyros island.

The variations of the atmospheric humidity, temperature and pressure cause the fluctuations of

the atmospheric refractive index. The atmosphere refractivity fluctuates between 288 and 388 for nights. This interval is shortening by 14% for day periods. In heavy precipitation phenomena ($R > 10 \text{ mm/h}$) refractivity values are between 317 and 363 with $N=340$ at the maximum R-value.



Figure 8. Measurements in moderate precipitation phenomena showed a power loss of about 10 to 12 dBm at 2,4 GHz

Measurements performed in a rainy day, for 40 minutes, with a wireless system at 2,4 GHz with minimum connection requirements approximately at -80 dBm. The first measurement was performed without rain, at free space and the signal's power was varied from -60 to -53 dBm. With the use of a directional antenna the receiving power was between -37 to -29 dBm. In the case of rain with R-value at 12 mm/h the signal's power varied in between -71 to -64 dBm. This 10 to 12 dBm attenuation was expected due to the path loss equation (4), [21] and measurements are in accordance with theoretical results.

7 CONCLUSION

Despite the fact that many fiber optic cable links have been installed in Greece, terrestrial or satellite microwave links play an important role in providing communication access to islands and rural or remote areas. The fast growth in telecommunications, increased demand for bandwidth, congestion in lower frequency bands and miniaturization of communication equipment have forced the designers to employ higher frequency bands such as the C (4 to 8 GHz), Ka (26.5 to 40 GHz), Ku (12 to 18 GHz) and V (40 to 75 GHz) bands. Rain is the most important factor for signal propagation deterioration in these frequencies. The contribution of rain attenuation to the quality of signal in these bands, needs to be studied. The aims of this paper are to estimate the magnitude of rain attenuation using the ITU-R model, carry out link performance analysis, and then propose reasonable, adequate fade margins that need to be applied for all provinces in Greece.

The EM wave propagation characteristics depend on atmospheric refractivity. Nevertheless, atmospheric refractivity varies in time and space randomly. Therefore the statistics of atmospheric refractivity and related propagation effects are of main interest. This work investigated the major differences between radio refractivity changes for Northwest Aegean Archipelagos. Radio refractivity values were calculated from measured

meteorological parameters (relative humidity, temperature and pressure) during a recent period of 4 years. The results showed that radio refractivity fluctuates between 288 and 388 but in strong precipitation phenomena where $R \geq 24 \text{ mm/h}$ it fluctuates in between 326 to 363 (N-units).

The rainfall rate exceeded for a probability of 0,01% of the average year and the location ($24,32^\circ \text{E}$, $38,50^\circ \text{N}$) is 48 mm/h and it is in accordance with previous published studies and ITU recommendations [22], [23]. Rainfall events with rain rates of 81, 48, 25 mm/h were observed in Skyros. The durations of these precipitations were 55 minutes, 80 minutes and 109 minutes respectively. The percentages of the time were 0.01 %, 0.015 % and 0,02 % respectively.

Incorporating data on extreme weather events like heavy precipitation impacts, into GIS maps would be of tactical advantage for military operations [24]. More measurements have to be performed for various conditions of precipitation. Moreover, the analysis of rainfall data of the longer period (of several decades) and several points must be carried out to determine the parameters involved in rain attenuation prediction.

ACKNOWLEDGMENTS

Authors would like to acknowledge the contribution of Hellenic National Meteorological Service, Division of Climatology-Applications for providing meteorological data used in this study.

REFERENCES

- [1] W.-Y. Chang, T.-C. C. Wang, P.-L. Lin, The Characteristics of Raindrop Size Distribution and Drop Shape Relation in Typhoon Systems from 2D-Video Disdrometer and NCU C-Band Polarimetric Radar, *Journal of Atmospheric and Oceanic Technology*, vol. 26, 2009
- [2] E. Villermaux, B. Bossa, Single-drop fragmentation determines size distribution of raindrops, *Nature Physics*, 2009.
- [3] J.S. Marshall, W.M. Palmer, The distribution of raindrops with size, *Journal of Meteorology*, 5, 1948.
- [4] R.A. Nelson, *Rain How it Affects the Communications Link*, Applied Technology Institute, 2000
- [5] B. Segal, The influence of rain gauge integration time on measured rainfall-intensity distribution functions," *Journal of Atmospheric and Oceanic Technology*, Vol. 3, 1986.
- [6] O. N. Okoro, G. A. Agbo, J. E. Ekpe and T. N. Obiekiezie, Comparison of hourly variations of radio refractivity for quiet and disturbed days during dry and rainy seasons at Minna, *International Journal of Basic and Applied Sciences*, vol. 2, 2013
- [7] Recommendation ITU-R P.1815-1, 2009, Differential rain attenuation.
- [8] M. Tamošiūnaitė, S. Tamošiūnas V. Daukšas M. Tamošiūnienė M. Žilinskas, Prediction of Electromagnetic Waves Attenuation due to Rain in the Localities of Lithuania, *Electronics and Electrical Engineering*, No. 9, 2010.
- [9] A. M. Burgueno, M. Puigcerver, and E. Vilar, Influence of rain gauge integration time on the rain rate statistics

- used in microwave communication, *Ann. Telecomm.*, Vol. 43, No. 9-10, 1988.
- [10] P. A. Owolawi, Rainfall Rate Probability Density Evaluation and Mapping for the Estimation of Rain Attenuation in South Africa and Surrounding Islands, *Progress In Electromagnetics Research*, Vol. 112, 2011
- [11] J. M. Gomez, *Satellite Broadcast Systems Engineering*, Artech House, 2002
- [12] Recommendation ITU-R P.838-3, Specific attenuation model for rain for use in prediction methods, 2005
- [13] R. L. Freeman, *Radio systems design for telecommunication*, Wiley, 2007
- [14] F. Moupfouma, L. Martin, Modelling of the rainfall rate cumulative distribution for the design of satellite and terrestrial communication systems, *International Journal of Satellite Communications and Networking*, v.13, 1995.
- [15] Recommendation ITU-R P.618-11, Propagation data and prediction methods required for the design of Earth-space telecommunication systems, 2013
- [16] Recommendation ITU-R P.676-10, Attenuation by atmospheric gases, 2013
- [17] R. Uijlenhoet, Raindrop size distributions and radar reflectivity-rain rate relationships for radar hydrology, *Hydrology and Earth System Sciences*, vol. 5, 2001.
- [18] J. Bosy W. Rohm J. Sierny J. Kaplon, GNSS Meteorology, *International Journal on Marine Navigation and Safety of Sea Transportation*, Vol. 5, 2011.
- [19] R. Crane, *Electromagnetic Wave Propagation through Rain*, Wiley, 1996
- [20] Recommendation ITU-R P.453-10, The Radio refractive index: its formula and refractivity data, 2012
- [21] E.A. Karagianni, A.P. Mitropoulos, A.G. Kavousanos-Kavousanakis, J.A. Koukös and M.E. Fafalios, Atmospheric Effects on EM Propagation and Weather Effects on the Performance of a Dual Band Antenna for WLAN Communications, *Nausivios Chora*, Volume 5, 2015, in press.
- [22] A. D. Papatsoris, K. Polimeris, I. Sklari, A. A. Lazou, Rainfall Characteristics for Radiowave Propagation Studies in Greece, *IEEE Antennas and Propagation Society International Symposium*, 2008.
- [23] Recommendation ITU-R P.837-6, Characteristics of precipitation for propagation modeling, 2012.
- [24] J. W. Weatherly and D. R. Hill, *The Impact of Climate and Extreme Weather Events on Military Operations*, ADA432260, 2004